

Role of mitochondria and network connectivity in intercellular calcium oscillations

I.V. Dokukina^a, M.E.Gracheva^b, E.A.Grachev^c, and J.D.Gunton^a

^aDepartment of Physics, Lehigh University, PA 18015, USA

^bUniversity of Illinois at Urbana-Champaign,
Beckman Institute for Advanced Science and Technology Urbana,
IL 61801, USA

^cFaculty of Physics, Moscow State University, Moscow, Russia

3rd July 2019

Abstract

Mitochondria are large-scale regulators of cytosolic calcium (Ca^{2+}) under normal cellular conditions. In this paper we model the complex behavior of mitochondrial calcium during the stimulation of a single cell by increase of agonist generated inositol 1,4,5-trisphosphate (IP_3) concentration and find results that are in good agreement with recent experimental studies. We also study the influence of the cellular network connectivity on intercellular calcium signaling via gap junction diffusion of second messengers. We include in our model the dependence of the junctional conductivity on the cytosolic calcium concentrations in adjacent cells. We consider three different mechanisms of calcium wave propagation through gap junctions: via Ca^{2+} diffusion, IP_3 diffusion, and both Ca^{2+} and IP_3 diffusion. Our results suggest that IP_3 diffusion is the mechanism of Ca^{2+} wave propagation and that Ca^{2+} diffusion is the mechanism of synchronization of cytosolic Ca^{2+} oscillations in adjacent cells. We also study the role of different topological configurations of cellular connectivity on these phenomena. We argue that the most important issue in modelling the intercellular calcium signaling is to account for the cellular topology of the tissue. Our results suggest that the dynamics of the tissue is defined by the topology of the connection graph of cells with each other.

Key words:Calcium wave, calcium signaling, inositol 1,4,5-trisphosphate, mitochondrion, gap junction, network, connectivity, topology.

E-mail addresses of all authors:

Irina V. Dokukina: irina.g@mail.ru

Maria E. Gracheva: gracheva@uiuc.edu

Eugene A. Grachev: grace@cmp.phys.msu.su

James D. Gunton: jdg4@lehigh.edu

Corresponding author: Irina V. Dokukina. Permanent address: Moscow State University, Faculty of Physics, building 2, room 2-40a, Leninskie Gory, Moscow, 119992, Russian Federation. Phone: 7-(095)-939-4178. E-mail address: irina_g@mail.ru.

1 Introduction

The capacity of mitochondria for accumulating cytosolic calcium (Ca^{2+}) down the electrical gradient generated by the respiratory chain has been known for several decades. However, the physiological significance of this phenomenon has been a subject of debate during much of the ensuing period. For a long time it was believed that the low affinity of the mitochondrial Ca^{2+} transporters, such as electrogenic uniporters and electroneutral antiporters, would allow a significant uptake only under conditions of dangerously high, cellular Ca^{2+} overload (for a review see Pozzan et al. (1994), Carafoli (2003)). In this case, there is a rapid mitochondrial accumulation of calcium, driven by the mitochondrial membrane potential and the fact that calcium possesses a very active electrogenic transport system. However, in recent years it has been shown that in some cells mitochondria do take up calcium ions at apparently physiological levels of calcium in the cytosol, thus establishing mitochondria as large-scale regulators of cytosolic Ca^{2+} under normal cellular conditions (Rizzuto et al., 1998), (Hajnoczky et al., 1995), (Thayer and Miller, 1990). Arnaudeau et al. (2001) showed that during stimulation with inositol 1,4,5-trisphosphate-generating agonists, HeLa cells maintain Ca^{2+} concentrations in the endoplasmic reticulum (ER) well above depleted levels, in phase with elevations of mitochondria and cytosolic Ca^{2+} concentration. The increase of the cytosolic Ca^{2+} concentration displayed an oscillatory behavior. A similar decrease of the ER Ca^{2+} concentration level during incubation with inositol 1,4,5-trisphosphate (IP_3) was observed in hepatocytes (Hajnoczky and Thomas, 1997), (Hajnoczky et al., 1999).

More complex results were obtained in other experiments. Kaftan et al. (2000) showed that mitochondria sequestered Ca^{2+} ions and tuned the frequency of oscillations of the cytosolic Ca^{2+} concentration in rat gonadotropes. Mitochondria accumulated Ca^{2+} rapidly and in phase with elevations of cytosolic Ca^{2+} concentration after gonadotropin-releasing hormone (GnRH) stimulation (binding of GnRH to its cell surface receptors) induced oscillations of cytosolic Ca^{2+} concentration. These oscillations are driven primarily by the release and re-uptake of Ca^{2+} from IP_3 -sensitive Ca^{2+} stores (Stojilkovic et al., 1994), (Hille et al., 1995). The mitochondrial Ca^{2+} concentration continued to increase over the course of several oscillations and remained elevated for many minutes, even after the oscillations ceased and the cytosolic Ca^{2+} concentration returned to near basal levels. Furthermore, it was found that inhibiting the mitochondrial Ca^{2+} uptake by the protonophore carbonyl cyanide *m*-chlorophenylhydrazone (CCCP), which should collapse the mitochondrial membrane potential and eliminate the electrical driving force for mitochondrial Ca^{2+} uptake, reduced the frequency and increased the amplitude and spike width of

GnRH-induced oscillations of cytosolic Ca^{2+} concentration.

A few theoretical studies exist whose goal is to understand better the contribution of the mitochondrion to intracellular calcium signaling and the effect of this signaling on mitochondrial function. Meyer and Stryer (1988) were the first to include mitochondria in a model of intracellular calcium signaling. Subsequently Marhl et al. (1998) showed that mitochondria played a role in the regulation of the amplitude during Ca^{2+} oscillations.

In this study we expand the model of intracellular Ca^{2+} oscillations proposed by Marhl et al. (2000) to better understand the physiological role of mitochondrial and cytosolic proteins. We believe it is important to take into account the cell transmembrane Ca^{2+} fluxes to understand the experiments by (Kaftan et al., 2000). In other words, our model is an "open-cell model". It is important to note that the importance of such fluxes on the intracellular calcium dynamics depends on the particular type of biological cell involved. For example, it has been shown experimentally that such fluxes do not play a significant role in the intracellular dynamics in airway smooth muscle cells (Roux and Marhl, 2000). In addition, the closed-cell model proposed by Marhl et al. (2000) successfully describes the intracellular dynamics of calcium upon stimulation of the cell by caffeine. A general discussion of the possible importance of transmembrane calcium fluxes is given in (Dupont et al., 2000a), (Schuster et al., 2002), (Falcke, 2004). The results of our analysis suggest that these transmembrane fluxes do play a role, however, in explaining significant features of the experimental results for pituitary gonadotropes (Kaftan et al., 2000).

Waves of increased free calcium concentration are one important mechanism whereby cells can coordinate their behavior with that of their neighbors, and are seen in a variety of cell types. Often such waves travel from cell to cell in a oscillatory manner, thus forming periodic intercellular calcium waves (Clair et al., 2001), (Evans and Sanderson, 1999). The mechanisms underlying such periodic intercellular waves are not well understood in any cell type. Sneyd et al. (1995) hypothesized that the diffusion of IP_3 through gap junctions was responsible for the propagation of intercellular calcium waves. This idea also was used in a model of intercellular calcium waves in hepatocytes (Dupont et al., 2000b). Alternative models of intercellular calcium waves in hepatocytes were based on the diffusion of cytosolic calcium through gap junctions (Hoefer, 1999) and on the action of calcium as a second messenger in paracrine signal transduction (Gracheva and Gunton, 2003). Stochastic versions of all these models are given by Gracheva et al. (2001), Gracheva and Gunton (2003). In all these models the junctional permeability was chosen to be a constant parameter. However, since calcium ions can close gap junctions (Bennett and Verselis, 1992), (Saez et al., 1993), this would appear to pose an obstacle to the propagation of intercellular Ca^{2+} waves via gap junctions. Fortunately, this apparent paradox can be resolved by considering the temporal aspects of these responses. It is known that extended exposure to high concentrations of Ca^{2+} ($> 10\mu M$) results in the closure of gap junctions (Bennett and Verselis, 1992), (Saez et al., 1993). It also appears that physiological concentrations of Ca^{2+} can reversibly close gap junctions but this response takes about 40s (Lazrak et al., 1994). Thus, because

Ca^{2+} waves propagate faster than the proposed closure times (Sanderson et al., 1990), the two possible intercellular messengers (Ca^{2+} and IP_3) (Saez et al., 1989), (Niessen et al., 2000) can diffuse to adjacent cells to propagate the wave before Ca^{2+} closes the gap junctions. Therefore, it would seem that a more accurate description of the gap junction permeability requires taking into account its dependence on the cytosolic calcium concentration, rather than treating it as a constant as in the earlier models (Dupont et al., 2000b), (Hoefer, 1999), (Gracheva et al., 2001).

In a second part of our paper we extend our model to include gap junction tunnelling between several coupled cells, to study the role of IP_3 and Ca^{2+} diffusion in wave propagation and intercellular synchronization. We believe that the most important issue in modelling intercellular calcium signaling is to account for the cellular topology of a tissue. As a rule, flat tissues are modelled in the form of a two-dimensional square grid (Sneyd et al., 1995), (Hoefer et al., 2002). However, in reality, the structure of even flat tissues is significantly more complicated. Even small areas of tissue can exhibit different topological types of cell connections between each other (Evans and Sanderson, 1999), (Niessen et al., 2000). In addition, in the case of local stimulation in which only one cell (not the entire tissue) is stimulated, it is important to know which cell is stimulated (for the same structure of cell connections). Thus in this paper we investigate the relation between the topology of cellular connectivity in flat tissue and the corresponding intercellular calcium signaling.

The outline of the paper is as follows. In section 2 we describe the model for a single cell, which involves several coupled differential equations for the global concentrations of Ca^{2+} in the endoplasmic reticulum, mitochondria and cytosol, as well as buffering proteins in the cytosol. IP_3 is the control parameter for the system, and is assumed to be produced by an external stimulus not treated explicitly in the model. In the following section 3 we describe the extension of the model to include gap junction coupling between several nearby cells. In sections 4 and 5 we discuss the results for the single and coupled cells, respectively, comparing our simulation results with several experimental studies. Finally in section 6 we provide a short conclusion, including directions for future work.

2 Description of the model

2.1 Schematic description

A schematic description of the model is presented in Fig. 1. There are three areas shown, the *Cyt* (cytosol), the *ER* (endoplasmic reticulum), and the *Mit* (mitochondria), as well as five variables, Pr (the concentration of free Ca^{2+} binding sites on the cytosolic proteins), $CaPr$ (the concentration of bounded Ca^{2+} binding sites on the cytosolic proteins), Ca_{cyt} (the concentration of Ca^{2+} in cytosol), Ca_{ER} (the concentration of Ca^{2+} in endoplasmic reticulum), and Ca_m (the concentration of Ca^{2+} in mitochondria). Thus the interactions between cytosolic, mitochondria and ER Ca^{2+} are included in the model. The

influence of cytosolic Ca^{2+} -binding proteins on intracellular calcium oscillations in the model is also included. Finally, we include in the model the influence of fluxes through the plasma membrane of the cell, since we believe that these fluxes play an important role in certain types of cells, for example, pituitary gonadotropes (Kaftan et al., 2000).

In the model of Marhl et al. (2000) control parameter k_{ch} represents the maximal permeability of the Ca^{2+} channels in the ER membrane. However, agonist generated IP_3 -mediated Ca^{2+} release from ER plays a fundamental role in many cell signaling processes. Therefore we add to the model the effect of IP_3 on the system by changing k_{ch} to a function $k_{ch}(IP_3)$, where IP_3 is the concentration of inositol 1,4,5-trisphosphate in the cell. Also the Ca^{2+} entry through the plasma membrane into the cell depends on IP_3 (see Table 1). The effect of IP_3 on the system is described by trapezoidal impulses of different amplitudes, which corresponds to external stimuli of different concentrations of agonists. Modelling the agonist generated IP_3 concentration by trapezoids is a numerically convenient form, rather than using a square impulse, for example.

One particularly useful aspect of the model is that it is constructed using a modular approach (Fall and Keizer, 2001). Thus, individual mechanisms were developed and tested against experimental data. We want to emphasize, therefore, that the modular construction of the model makes it relatively easy to exchange particular mechanisms or to extend the model with features that have not been included as part of this work.

2.2 Summary of the model

- We used the Marhl et al. (2000) model as the basis for the mitochondrial and ER functions.
- We incorporated the Hoefer et al. (2002) model for ionic fluxes through the plasma membrane of the cell.
- Due to the ionic fluxes through the plasma membrane of cell the system is open and the conservation law for the total cellular calcium concentration fails. Therefore we formulate the time dependence of $CaPr$ in terms of explicit differential equation.
- We suppose that k_{ch} (cf. Marhl et al. (2000)) is a smooth monotone increasing function of IP_3 , which we choose as a linear function, as a first approximation. That is, we assume a linear dependence $k_{ch}IP_3 + IP_{3_0}$, where $IP_{3_0} = const$. This is not completely realistic, since in the case of $IP_3 = 0$ there is no essential release of calcium from the ER. In addition, we do not find any significant differences between the results for $IP_{3_0} = 0$ and $IP_{3_0} \neq 0$. Therefore we put for simplicity $IP_{3_0} = 0$, so that $k_{ch}(IP_3) = k_{ch} \cdot IP_3$. In order to improve the approximation for $k_{ch}(IP_3)$, we would need experimental input that is currently not available.

2.3 Model fluxes and differential equations

All the fluxes incorporated into this model are shown in Fig. 1. The Ca^{2+} entry rate expression accounts for a small leak flux that is always present and an agonist-dependent influx, which can be receptor-operated or store-operated Ca^{2+} influx, or both (Dupont and Goldbeter, 1993). For simplicity, the latter is made a function of IP_3 concentration as a measure of the agonist dose (see J_{in} in Table 1). Calcium extrusion is modelled by a linear rate law (see J_{out} in Table 1).

Two different calcium fluxes for the ER are included in the model: the ATP-dependent calcium uptake from the cytosol into the ER (see J_{serca} in Table 1) and the Ca^{2+} efflux from the ER through channels following the calcium-induced calcium release (CICR) mechanism with an additional Ca^{2+} leak flux from the ER into the cytosol (see J_{rel} in Table 1).

The exchange of Ca^{2+} between the mitochondria and the cytosol is described by the following Ca^{2+} fluxes: an active Ca^{2+} uptake by mitochondrial uniporters (see J_{mi} in Table 1), calcium release through Na^+/Ca^{2+} exchangers combined with a flux through the mitochondrial permeability transition pores (PTPs) and a very small non-specific leak flux (see J_{mo} in Table 1). The complete expressions for these fluxes are given in Table 1.

The evolution of the system is governed by the following differential equations (for parameter values see Table 2):

$$\frac{dCa_{cyt}}{dt} = J_{in} - J_{out} + J_{rel} - J_{serca} + J_{mo} - J_{mi} + k_- CaPr - k_+ Ca_{cyt}Pr, \quad (1)$$

$$\frac{dCa_{ER}}{dt} = \frac{\beta_{ER}}{\rho_{ER}}(J_{serca} - J_{rel}), \quad (2)$$

$$\frac{dCa_m}{dt} = \frac{\beta_m}{\rho_m}(J_{mi} - J_{mo}), \quad (3)$$

$$\frac{dCaPr}{dt} = k_+ Ca_{cyt}Pr - k_- CaPr, \quad (4)$$

and following conservation relation for the total concentration of free and bounded Ca^{2+} -binding sites on the cytosolic proteins:

$$Pr_{tot} = Pr + CaPr. \quad (5)$$

Note that we have described the mitochondrial and ER buffers via a buffering constant, β , whereas we have described the cytosolic buffers dynamically. We have chosen the approximation for the mitochondrial and ER buffers for simplicity; we plan to develop a dynamical description of this buffering in a subsequent study.

3 Model of gap junctions between cells

We now extend our model to include gap junction tunneling between nearby cells. We choose the junctional conductivity to be the following function of the cytosolic calcium concentration difference between adjacent cells i and j :

$$\gamma_{Ca(ij)} = k_{gap} \frac{k_{Ca(ij)}^5}{Ca_{cytMax(ij)}^5 + k_G^5}. \quad (6)$$

We also choose the junctional conductivity for IP_3 between adjacent cells i and j to be

$$\gamma_{IP(ij)} = k_{gap} \frac{k_{IP(ij)}^5}{Ca_{cytMax(ij)}^5 + k_G^5}, \quad (7)$$

where $Ca_{cytMax(ij)}$ is the maximum concentration of cytosolic calcium between cells i and j . For other parameters see Table 2.

In this case the system of equations that describes calcium wave propagation between several (2-3) cells is

$$\begin{aligned} \frac{dCa_{cyt(i)}}{dt} = & J_{in} - J_{out} + J_{rel} - J_{serca} + J_{mo} - J_{mi} + \\ & + k_- CaPr_{(i)} - k_+ Ca_{cyt(i)} Pr_{(i)} + \\ & + \gamma_{Ca(ij)} (Ca_{cyt(j)} - Ca_{cyt(i)}) + \gamma_{Ca(ik)} (Ca_{cyt(k)} - Ca_{cyt(i)}), \end{aligned} \quad (8)$$

$$\frac{dCa_{ER(i)}}{dt} = \frac{\beta_{ER}}{\rho_{ER}} (J_{serca} - J_{rel}), \quad (9)$$

$$\frac{dCa_{m(i)}}{dt} = \frac{\beta_m}{\rho_m} (J_{mi} - J_{mo}), \quad (10)$$

$$\frac{dCaPr_{(i)}}{dt} = k_+ Ca_{cyt(i)} Pr_{(i)} - k_- CaPr_{(i)}, \quad (11)$$

$$Pr_{tot(i)} = Pr_{(i)} + CaPr_{(i)}, \quad (12)$$

$$\frac{dIP_{3(i)}}{dt} = -J_{deg} + \gamma_{IP(ij)} (IP_{3(j)} - IP_{3(i)}) + \gamma_{IP(ik)} (IP_{3(k)} - IP_{3(i)}), \quad (13)$$

where indices i , j and k denote the cell number.

The case in which the index pairs $(ijk) = (120) = (210)$ with $k_{Ca(13)} = k_{Ca(23)} = 0$ and $k_{IP(13)} = k_{IP(23)} = 0$ corresponds to just two coupled cells. Also the case in which $(ijk) = (100)$, $Ca_{cytMax(ij)} = Ca_{cyt(1)}$ and all junctional coefficients are equal to zero corresponds to only one cell, which is equivalent to equations (1)-(5). It is also worth noting that in the case of index pairs $(ijk) = (123) = (213) = (312)$ there are three possible different configurations

of three coupled cells. If $k_{Ca(13)} = k_{IP(13)} = 0$, we have a one-dimensional chain of cells, with the first cell interacting only with the second cell, the second cell interacting with both the first and third cells and the third cell interacting only with the second cell (see Fig. 2 A). The same line chain with other order of cells is shown in Fig. 2 B. If none of the junctional coefficients vanish, each cell interacts with two other cells (see Fig. 2 C). The right side of Fig. 2 shows graphs that correspond to these three configurations.

The system can be easily generated to the case of more than three cells. For example, all configurations in two dimensions of four coupled cells are shown in Fig. 3. All these are biologically realistic in two dimensions. Examples of real cellular configurations *in vitro* are shown in Fig. 1 and 2 in (Niessen et al., 2000) and Fig. 9 and 11 in (Evans and Sanderson, 1999). The system of cells 1, 2, 3, 7 in Fig. 1a in (Niessen et al., 2000) (if the rest cells are removed) corresponds to the topological configuration in Fig. 3 A (cell 3 or 7 should be stimulated) and 3 B (cell 1 or 2 should be stimulated) in our study. The system of cells 1, 2, 5, 7 in Fig. 1a in (Niessen et al., 2000) (if the rest cells are removed) corresponds to the topological configuration in Fig. 3 C (cell 5 should be stimulated), 3 D (cell 2 or 7 should be stimulated) and 3 E (cell 1 should be stimulated) in our study. The system of cells 1, 3, 5, 7 in Fig. 1a in (Niessen et al., 2000) (if the rest cells are removed) corresponds to the topological configuration in Fig. 3 F (cell 1 should be stimulated) and 3 G (cell 3, 5 or 7 should be stimulated) and the system of cells in Fig. 9 in (Evans and Sanderson, 1999) corresponds to the topological configuration in Fig. 3 F (cell B should be stimulated) and 3 G (cell A, C or D should be stimulated) in our study. The systems of cells in Fig. 1c and Fig. 2 in (Niessen et al., 2000) and in Fig. 11 in (Evans and Sanderson, 1999) corresponds to the topological configuration in Fig. 3 I and 3 J in present paper. Finally, we believe that it is possible to extract the configuration shown in Fig. 3 H from a variety of cellular tissues. We consider only two-dimensional configurations of cells in this paper, since calcium signaling in three-dimensional tissues is a separate subject (which we plan to study in the future).

It is also important to note that in order to model Ca^{2+} wave propagation the IP_3 stimulus (which mimics the mechanical stimulation or local application of a stimulus) is applied only to the first cell. We model this IP_3 stimulus as a trapezoidal function of time for the first cell. Also, in the modelling of intercellular calcium signaling we add to the model a term describing the degradation of IP_3 (Sneyd et al., 1995) in each of the cells:

$$J_{deg} = \frac{V_p IP_3 k_p}{k_p + IP_3}. \quad (14)$$

Without this term, the calcium levels reach unphysiological values in the asymptotic time limit (Sanderson et al., 1990). The values of all the parameters are given in Table 2.

In order to analyze the synchronization between cytosolic Ca^{2+} in two coupled cells we introduce the similarity function $S(\tau)$, which characterizes the lag

synchronization (Rosenblum et al., 1997):

$$S^2(\tau) = \frac{\langle [Ca_{cyt(2)}(t + \tau) - Ca_{cyt(1)}(t)]^2 \rangle}{[\langle Ca_{cyt(1)}^2(t) \rangle \langle Ca_{cyt(2)}^2(t) \rangle]^{1/2}}, \quad (15)$$

where τ is the time shift. If the signals $Ca_{cyt(1)}$ and $Ca_{cyt(2)}$ are independent, the time averaged difference between them is of the same order as the signals themselves (respectively $S(\tau) \sim 1$ for all τ). If $Ca_{cyt(1)}(t) = Ca_{cyt(2)}(t)$, as in the case of complete synchronization, $S(\tau)$ reaches its minimum $\min_{\tau} S(\tau) = 0$ for $\tau = 0$.

4 Results for single cell

First of all, we calculate the ratio between the amplitudes of the increase of calcium concentrations in the mitochondria and cytosol, and also study their synchronization. As expected (Rizzuto et al., 2000), during a brief stimulation of cell by increase in IP_3 (resulting from an external stimulus), there was an increase in Ca_{cyt} , simultaneously with an increase in Ca_m ; Ca_m exceeded that of Ca_{cyt} by an order of magnitude (see Fig. 4). We also find a decrease of the Ca_{ER} level during a prolonged stimulation of cell by IP_3 (see Fig. 5). It is very realistic, because Ca^{2+} is released from the ER in cytosol and mitochondria during stimulation of cell and is restored in the ER after the end of stimulation. At the same time, Ca_m rapidly increases, in phase with the oscillatory increase of Ca_{cyt} and a concomitant decrease of Ca_{ER} ; the Ca_m level remains elevated for about four minutes even after the oscillations have ceased and Ca_{cyt} has returned to its basal level (see Fig. 5), consistent with previous observations (cf. Fig. 3 in Kaftan et al. (2000)).

In Kaftan et al. (2000) the protonophore CCCP was added, which should collapse the mitochondrial membrane potential and eliminate the electrical driving force for mitochondrial Ca^{2+} uptake. In this case, an application of CCCP during periodic Ca^{2+} oscillations dramatically slowed the rate of each downstroke of Ca_{cyt} and reduced the frequency of oscillations. Also, the amplitude and spike width of cytosolic Ca^{2+} are much larger during the application of CCCP than before and after the application. In our model, the procedure of application of CCCP is equivalent to setting $k_{mi} = 0$. Accordingly, we find that while $k_{mi} = 0$ (peak B, Fig. 6) the spike width and amplitude of Ca_{cyt} oscillations are significantly larger than the corresponding behavior for the usual value of $k_{mi} = 300 \mu M \cdot s^{-1}$ (peaks A and C, Fig. 6), which is in good agreement with the experiment Kaftan et al. (2000). (For better illustration the peaks A, B and C in Fig. 6 were shifted and overlaid so that the maxima of cytosol Ca^{2+} concentration occur at the same time).

In the experiment of Kaftan et al. (2000) the frequency of Ca_{cyt} oscillation decreased during the application of protonophore CCCP (cf. Fig. 1 in Kaftan et al. (2000)); also there was an increase in the basal level of cytosolic calcium. Both of these return to previous levels after the withdrawal of CCCP.

We believe that the reason for both of these changes is that the cell is of finite (non-zero) size, rather than point-like as described in the model. In reality, the mitochondria, ER and plasma membrane are separated spatially and the concentration of calcium and other variables in a cell are spatially dependent. It seems that during the collapse of the mitochondrial membrane potential by CCCP there is an area of elevated calcium concentration near the mitochondria which cannot be reduced quickly, since calcium needs a finite time to reach the calcium pumps in the cell plasma membrane and the ER. This is the reason leading to the observation of an elevated basal level of cytosolic calcium. We cannot describe this effect since we do not take into account spatial effects in our model. The change in calcium oscillation frequency is also a result of these spatial effects. Obviously, the observed calcium oscillations result from the simultaneous operation of different dynamical processes, many of which are oscillatory in nature. During a long enough external stimulation of the cell, all these processes become synchronized (as in synchronization of the frequencies of coupled oscillators Pikovsky et al. (2001)); as a consequence calcium oscillations of a definite frequency and amplitude are observed. However, if one of these processes is switched off (as during a total suppression of the fast absorption of cytosolic calcium by mitochondrial uniporters) a temporary desynchronization of the system occurs, leading to a change in the frequency and amplitude of the oscillations. Since in reality the mitochondria, ER and plasma membrane are spaced out, the consequences of such a change in the system can be emulated only partially by our "one-point" model, which ignores such spatial variations within the cell. Our model does reproduce very well, however, the increase in the amplitude and the width of the calcium spike during the inhibition of the fast absorption of the calcium by mitochondria.

5 Results for coupled cells

We begin by discussing the case of two coupled cells. We consider three different mechanisms of signal transduction between adjacent cells: diffusion of only IP_3 , of only Ca^{2+} and of both IP_3 and Ca^{2+} through gap junctions between cells. In the case of only Ca^{2+} diffusion there is no calcium wave propagation between cells (these results are not shown). In the case of only IP_3 diffusion we find that calcium oscillations are generated in the second cell (see Fig. 7). Note that the total IP_3 in the cells is shown in Fig. 7. The total concentration of IP_3 in a cell includes the agonist generated IP_3 signal in trapezoid form, the decay of IP_3 (see J_d) and lowering of IP_3 concentration in a given cell with time due to diffusion into adjacent cells via gap junctions. In Fig. 7 the agonist generated IP_3 signal is applied from 200 s to 400 s in trapezoidal form with amplitude of $30 \mu M$. The increase of IP_3 concentration in stimulated cell after the withdrawal of stimulus at 400 s is due to the feedback between two adjacent cells.

The results of our investigation of possible synchronization between cytosolic Ca^{2+} in these two cells are shown in Fig. 8. Since synchronization between Ca^{2+}

oscillations in adjacent cells is not established immediately, we investigate the presence of synchronization for three periods of time (from 300s to 1000s, from 500s to 1000s and from 700s to 1000s) which differ by the time duration past from the onset of oscillations in the second cell.

In the case of only IP_3 diffusion between cells we find some dependence of the cytosolic calcium concentrations in the two cells on each other. However, the oscillations of calcium in the second cell are not synchronous with the calcium oscillations in the first cell.

Finally, when both Ca^{2+} and IP_3 diffuse we find not only calcium oscillations in neighboring cells, but in this case a complete synchronization between calcium oscillations in cells is established during about 400s after the onset of oscillations in the second cell (see Fig. 9).

Therefore we conclude that there are two separate mechanisms involved. In the first case, IP_3 diffusion provides the mechanism for calcium wave propagation between cells, as was proposed by (Sneyd et al., 1995). Diffusion of Ca^{2+} , however, is necessary (in addition to IP_3 diffusion), to synchronize the oscillations among the neighboring cells.

For more than two connected cells our results show that the propagation of calcium waves depends on the spatial configuration of cells. There are three possible configurations of interactions between three cells (see Fig. 2). If the location of the two neighboring cells is symmetric with respect to the first cell (Fig. 2 B, C), than one can see similar oscillations in both the second and third cells, following the initial delay of about 80 s from the onset of oscillations in the first cell. In the case of linear chain (Fig. 2 A) there is a difference in the calcium oscillations in the second and third cells. There is not only a delay time between the onset of calcium oscillations in the first and second cells, but also between the second and third cells (both delay times are about 80s). The value of this delay time differs from that found in (Sneyd et al., 1995), (Sanderson et al., 1990), which is due to the different choice of parameter values in the two studies.

Also, we briefly describe the results for the case of four connected cells. The results for all configurations of four cells are summarized in Table 3. We note that we study only in-plane (two-dimensional) cell configurations. It is possible to distinguish five different configurations of four cells on a plane. However, for the same topological configuration of cells, Ca^{2+} signaling greatly depends on which cell in the structure was stimulated. Taking into account this issue we identify ten cell configurations. Similarly to the case of three cells, the dynamics of Ca^{2+} in cells symmetrically positioned with respect to the simulated cell is identical, for example, see configurations A, B, C, E, F, G, H and I in Fig. 3. This holds while all cells in configurations are indistinguishable. Also, this assumption allows to study the intercellular Ca^{2+} signaling only on topology of the cell to cell connections in a given cell configuration. The investigation of the dynamics of cell-cell Ca^{2+} signaling in configurations comprised of cells with different properties is a more complicated problem, and thus, is a subject of our future research.

We now describe the key features of signaling in four cell configurations

in more detail. For example, in the case of configuration H the first cell has two connections with adjacent cells (there are four connections between cells altogether) and we find very good calcium wave propagation between cells. Also, the dynamics of Ca^{2+} in cells 2 and 3, which are positioned symmetrically with respect to the stimulated cell 1, is the same (see Table 3). The delay time between the onset of Ca^{2+} oscillations in the stimulated cell and the beginning of oscillations in all other cells in configuration depends on the order number of neighbor of a given cell. In the case of a direct connection with the first simulated cell (first order neighbors) the delay time varies from 56 s to 91 s (see Table 3). For example, in configuration I cell 2 is the first order neighbor of cell 1. For the second order neighbor there is one additional cell between the stimulated cell and a given cell. For example, in configuration I cell 3 is the second order neighbor for cell 1. For the second order neighbors the time delay for onset Ca^{2+} oscillation varies from 133 s to 271 s which is significantly larger than in the case of the first order neighbors. Besides, for the second order neighbors there is a difference in dynamics depending on the presence or absence of connections with other second order neighbors (compare cell 3 and cell 4 in configurations C and G). For in-plane configurations of four cells there is only one neighbor of third order which is present in configuration I. For the given parameters there are no oscillations in cell 4 of configuration I, as indicated in Table 3.

Thus, each cell configuration can be characterized by a definite set of neighbors of each order, moreover the propagation of intercellular Ca^{2+} wave for each configuration depends on this set. According to the set of neighbors all cell configurations can be divided into four classes:

- one neighbor of first order, one neighbor of second order, one neighbor of third order (configuration I);
- one neighbor of first order, two neighbors of second order (configurations C, G);
- two neighbors of first order, one neighbor of second order (configurations A, D, H, J);
- three neighbors of first order (configurations B, E, F).

The fast decline of intercellular Ca^{2+} wave is characteristic of the first two classes, whereas a steady expansion of intercellular Ca^{2+} waves is characteristic of the last two classes (see Table 3).

For example, in the case of configuration C the first cell has only one connection with another cell (there are four connections between all cells, as in H) and this results in a decreased range of the calcium wave propagation from the first cell. There is an even stronger decrease of the range of wave propagation in the case of configuration I, which is a linear chain of four cells.

Results for configuration J (the most unsymmetrical of the configurations) are shown in Fig. 10, as example. The first three oscillations in Ca_{cyt} in the cell 1 are induced by external agonist generated IP_3 (from 200s to 400 s),

the next five oscillations result from the increase of IP_3 due to the feed back between cells (from 400s to 1000s). In configuration J cells 2 and 3 are located symmetrically with respect to cell 1 (see Fig. 3 J); however, some part of the IP_3 that originates in cell 3 from cell 1 escapes to cell 4. This is the reason why in cell 3 the calcium oscillations occur after those in cell 2.

Thus, the results of our analysis for this model suggest that the topology of connections between cells plays an important role in calcium wave propagation in flat cell tissues.

6 Conclusion

In this study, we demonstrate the importance of the mitochondria in both intracellular and intercellular calcium oscillations. Our model produces results that are in good agreement with experimental studies, as noted in Section 4. Our model shows the main features of intracellular calcium signaling, including the fact that during cytosolic calcium oscillations the concentration of calcium in the ER decreases while the concentration of mitochondrial calcium increases. Also, in our model the mitochondrion accumulates calcium rapidly and in phase with the oscillatory elevations of cytosolic calcium. Furthermore, the mitochondrial calcium concentration remains elevated for many minutes after the withdrawal of IP_3 stimulation and after calcium oscillations in cytosol vanish, as seen experimentally (Kaftan et al., 2000). It is also worth noting that the collapse of the mitochondrial calcium uptake in our model significantly increases the spike width, amplitude and frequency of cytosolic calcium oscillations as compared with its behavior for the normal case (Kaftan et al., 2000).

We also studied different possible mechanisms of intercellular calcium signaling. In epithelial cell cultures, for example, a mechanically stimulated intercellular calcium wave appears to propagate via the intercellular diffusion of the IP_3 (Sneyd et al., 1995). In hepatocytes, oscillatory intercellular Ca^{2+} waves appear to be generated by the coupling of intracellular Ca^{2+} oscillations (Dupont et al., 2000b), (Hoefer, 1999). A plausible hypothesis is that these waves are the result of intercellular coupling by means of the diffusion of Ca^{2+} through gap junctions (Hoefer, 1999). Since both calcium and IP_3 can act as intercellular messengers (Evans and Sanderson, 1999), we considered all three possibilities: diffusion of only Ca^{2+} , only IP_3 and both Ca^{2+} and IP_3 through gap junctions. In the case in which Ca^{2+} is the only messenger, there is no formation of intercellular calcium wave at all. In the case in which IP_3 is the only messenger, there is a propagation of calcium wave, but the oscillations of cytosolic calcium in cells adjacent to the stimulated cell are not in synchrony with the oscillations in the perturbed cell. Finally, when both calcium and IP_3 diffuse there is calcium wave propagation with completely synchronous oscillations in each cell from about 400 s after the onset of oscillations in the perturbed cell. Therefore we conclude that within the context of our model, diffusion of calcium through gap junctions is responsible for the synchronization of calcium oscillations in adjacent cells. However, it is not the reason for calcium wave propagation in cell networks.

Correspondingly, the diffusion of IP_3 is the mechanism for intercellular calcium wave propagation.

We also studied the dependence of intercellular signaling on the topological configurations of cell connectivity, and found results that can be understood intuitively. The order number of neighbors also has an influence on the amplitude of the propagating wave, as discussed in Section 5.

While modelling the intercellular calcium signaling it is necessary to recognize that the transition from one cell to tissue is not a simple quantitative conversion. It is not a transition from one cell to a chain of cells or some grid of cells, but it is a more complex transition defined by the topology of tissue. We have shown that the dynamics of tissue in small areas (and also in larger regions – I.V. Dokukina, A.A. Tsukanov, M.E. Gracheva, E.A. Grachev, unpublished results) is defined not by a chain or grid of cells, but by the topology of the connection graph of cells with each other. It is possible to judge the tissue topology from the dynamics of signaling; in turn, the tissue topology can change the intercellular signaling dynamics, enforcing its own rhythm. Thus, the intercellular dynamics of calcium and the corresponding topology of cell connections form an unbroken, complete system.

Finally, in our study of the role of network connectivity between cells we considered only the case in which all cells have the same parameters. It would be interesting to study situations in which there is a variation in cellular sensitivity to agonist (Evans and Sanderson, 1999) and in gap junction conductivities. These are subjects of future research.

7 Acknowledgments

This research was supported in part by grants from the National Science Foundation (DMR0302598), and the G. Harold and Leila Y. Mathers Charitable Foundation.

References

Arnaudeau, S., Kelley, W.L., Walsh, J.V., Demaurex, Jr., Demaurex, N., 2001. Mitochondria recycle Ca^{2+} to the endoplasmic reticulum and prevent the depletion of neighboring endoplasmic reticulum regions. *J. Biol. Chem.* 276(31), 29430-29439.

Bennett, M.V.L., Verselis, V.K., 1992. Biophysics of gap junctions. *Semin. Cell. Biol.* 3, 29-47.

Carafoli, E., 2003. Historical review: mitochondria and calcium: ups and downs of an unusual relationship. *TRENDS in Biochem. Sci.* 28(4), 175-181.

Clair, C., Chalumeau, C., Tordjmann, T., Poggiali, J., Erneux, C., Dupont, G., Combettes, L., 2001. Investigation of the roles of Ca^{2+} and $InsP_3$ diffusion in the coordination of Ca^{2+} signals between connected hepatocytes. *J. Cell Sci.* 114, 1999-2007.

Dupont, G., Goldbeter, A., 1993. One-pool model for Ca^{2+} oscillations involving Ca^{2+} and inositol 1,4,5-triphosphate as co-agonists for Ca^{2+} release. *Cell Calcium.* 14, 311-322.

Dupont, G., Swillens, S., Clair, C., Tordjmann, T., Combettes, L., 2000a. Hierarchical organization of calcium signals in hepatocytes: from experiments to models. *Biochim. Biophys. Acta.* 1498, 134-152.

Dupont, G., Tordjmann, Th., Clair, C., Swillens, St., Claret, M., Combettes., L., 2000b. Mechanism of receptor-oriented intercellular calcium wave propagation in hepatocytes. *FASEB J.* 14, 279-289.

Evans, J.H., Sanderson, M.J., 1999. Intracellular calcium oscillations induced by ATP in airway epithelial cells. *Am. J. Physiol.* 277 (Lung Cell. Mol. Physiol. 21), L30-L41.

Falcke, M., 2004. Reading the patterns in living cells the physics of Ca^{2+} signaling. *Adv. Phys.* 53(3), 255-440.

Fall, C.P., Keizer, J.E., 2001. Mitochondrial modulation of intracellular Ca^{2+} signaling. *J. Theor. Biol.* 210, 151-165.

Gracheva, M.E., Toral, R., Gunton, J.D., 2001. Stochastic effects in intercellular calcium spiking in hepatocytes. *J. Theor. Biol.* 212, 111-125.

Gracheva, M.E., Gunton, J.D., 2003. Intercellular communication via intracellular calcium oscillations. *J. Theor. Biol.* 221, 513-518.

Hajnoczky, G., Robb-Gaspers, L.D., Seitz, M.B., Thomas, A.P., 1995. Decoding of cytosolic calcium oscillations in the mitochondria. *Cell.* 82, 415-424.

Hajnoczky, G., Thomas, A.P., 1997. Minimal requirements for calcium oscillations driven by the IP_3 receptor. *EMBO J.* 16(12), 3533-3543.

Hajnoczky, G., Hager, R., Thomas, A.P., 1999. Mitochondria suppress local feedback activation of inositol 1,4,5-trisphosphate receptors by Ca^{2+} . *J. Biol. Chem.* 274(20), 14157-14162.

Hille, B., Tse, A., Tse, F.W., Bosma, M.M., 1995. Signaling mechanisms during the response of pituitary gonadotropes to GnRH. *Recent Prog. Horm. Res.* 50, 7595.

Hoefer, Th., 1999. Model of intercellular calcium oscillations in hepatocytes: synchronization of heterogeneous cells. *Biophys. J.* 77, 1244-1256.

Hoefer, T., Venance, L., Giaume, C., 2002. Control and plasticity of intercellular calcium waves in astrocytes: a modeling approach. *J. Neurosci.* 22(12), 4850-4859.

Kaftan, E.J., Xu, T., Abercrombie, R.F., Hille, B., 2000. Mitochondria shape hormonally induced cytoplasmic calcium oscillations and modulate exocytosis. *J. Biol. Chem.* 275(33), 25465-25470.

Lazrak, A., Peres, A., Giovannardi, S., Peracchia, C., 1994. Ca-mediated and independent effects of arachidonic acid on gap junctions and Ca-independent effects of oleic acid and halothane. *Biophys. J.* 67, 1052-1059.

Marhl, M., Schuster, S., Brumen, M., 1998. Mitochondria as an important factor in the maintenance of constant amplitude of cytosolic calcium oscillations. *Biophys. Chem.* 71, 125-132.

Marhl, M., Haberichter, T., Brumen, M., Heinrich, R., 2000. Complex calcium oscillations and the role of mitochondria and cytosolic proteins. *BioSystems*. 57, 75-86.

Meyer, T., Stryer, L., 1988. Molecular model for receptor-stimulated calcium spiking. *Proc. Natl. Acad. Sci. USA.* 85, 5051-5055.

Niessen, H., Harz, H., Bedner, P., Kramer, K., Willecke, K., 2000. Selective permeability of different connexin channels to the second messenger inositol 1,4,5-trisphosphate. *J. Cell Sci.* 113, 1365-1372.

Pikovsky, A., Rosenblum, M., Kurths, J., 2001. Synchronization: a universal concept in nonlinear sciences. Cambridge University Press, Cambridge, UK.

Pozzan, T., Rizzuto, R., Volpe, P., Melodeshi, J., 1994. Molecular and cellular physiology of intracellular Ca^{2+} stores. *Physiol. Rev.* 74(3), 595-636.

Rizzuto, R., Pinton, P., Carrington, W., Fay, F.S., Fogarty, K.E., Lifshitz, L.S., Tuft, R.A., Pozzan, T., 1998. Close contacts with the endoplasmic reticulum as determinants of mitochondrial Ca^{2+} responses. *Science*. 280, 1763-1766.

Rizzuto, R., Bernardi, P., Pozzan, T., 2000. Mitochondria as all-round players of the calcium game. *J. Physiol.* 529, 37-47.

Rosenblum, M.G., Pikovsky, A.S., Kurths, J., 1997. From phase to lag synchronization in coupled chaotic oscillators. *Phys. Rev. Lett.* 78(22), 4193-4196.

Roux, E., Marhl, M., 2004. Role of sarcoplasmic reticulum and mitochondria in Ca^{2+} removal in airway myocytes. *Biophys. J.* 86, 2583-2595.

Saez, J.C., Connor, J.A., Spray, D.C., Bennett, V.L., 1989. Hepatocyte gap junctions are permeable to the second messenger, inositol 1,4,5-trisphosphate, and to calcium ions. *Proc. Natl. Acad. Sci. USA.* 86, 2708-2712.

Saez, J.C., Berthoud, V.M., Moreno, A.P., Spray, D.C., 1993. Gap junctions. Multiplicity of controls in differentiated and undifferentiated cells and possible functional implications. In: Shenolikar, S., Nairn, A.C. (eds). *Advances in second messenger and phosphoprotein research*. Raven Press. New York. 27, 163-198.

Sanderson, M.J., Charles, A.C., Dirksen, E.R., 1990. Mechanical stimulation and intercellular communication increases intracellular Ca^{2+} in epithelial cells. *Cell regulation.* 1, 585-596.

Schuster, S., Marhl, M., Hoefer, Th., 2002. Modeling of simple and complex calcium oscillations. *Eur. J. Biochem.* 269, 1333-1355.

Sneyd, J., Wetton, B.T.R., Charles, A.C., Sanderson, M.J., 1995. Intercellular calcium waves, mediated by diffusion of inositol (1,4,5)-trisphosphate: a two dimensional model. *Am. J. Physiol.* 268, C1537-C1545.

Stojilkovic, S.S., Reinhart, J., Catt, K.J., 1994. Gonadotropin-releasing hormone receptors: structure and signal transduction pathways. *Endocr. Rev.* 15, 462-499.

Thayer, S.A., Miller, R.J., 1990. Regulation of intracellular free calcium concentration in single rat dorsal root ganglion neurons in vitro. *J. Physiol.* 425, 85-115.

Figure Captions

Fig. 1. Schematic representation of the model.

Fig. 2. Different structures of connections between three cells. Grey color of cell 1 means that this cell is stimulated. The right side shows graphs that correspond to each configuration.

Fig. 3. Different structures of connections between four cells. Grey color of cell 1 means that this cell is stimulated. The right side shows graphs that correspond to each cell configuration.

Fig. 4. IP_3 -dependent decrease of Ca^{2+} concentration in ER (Ca_{ER}) and increase of cytosolic (Ca_{cyt}) and mitochondrial (Ca_m) Ca^{2+} concentrations. For all parameters see Table 2.

Fig. 5. Mitochondria rapidly accumulate Ca^{2+} during Ca_{cyt} oscillations. For all parameters see Table 2.

Fig. 6. Calcium oscillations due to collapse of the mitochondrial membrane potential. Peak A: typical calcium spike for the normal mitochondrial membrane potential before its collapse ($k_{mi} = 300\mu M \cdot s^{-1}$ from 0s to 50s). Peak B: typical calcium spike during collapse of the mitochondrial membrane potential. The amplitude and spike width are increased ($k_{mi} = 0$ from 50s to 100s). Peak C: typical calcium spike for the normal mitochondrial membrane potential after collapse. The amplitude and spike width of the Ca_{cyt} oscillations are decreased in comparison with the period of collapse ($k_{mi} = 300\mu M \cdot s^{-1}$ from 100s to 150s). *Top panel*: Ca_{cyt} oscillations with marked peaks A, B and C. IP_3 is constant, with $IP_3 = 50\mu M$; values of the other parameters are given in Table 2. *Bottom panel*: the peaks A, B and C were shifted and overlaid so that the maxima of cytosol Ca^{2+} concentration occur at the same time. An increase of the amplitude and the spike width of peak B in comparison with peaks A and C can be seen.

Fig. 7. Intercellular calcium signaling between two cells based on diffusion of only IP_3 through gap junctions. For all parameters see Table 2.

Fig. 8. Similarity function for calcium oscillations between two coupled cells based on diffusion of only IP_3 through gap junctions. There is no synchronization between Ca^{2+} oscillations in two coupled cells. For all parameters see Table 2.

Fig. 9. Similarity function for calcium oscillations between two coupled cells based on diffusion of both IP_3 and Ca^{2+} through gap junctions. There is synchronization between cytosolic Ca^{2+} oscillations in two coupled cells. For all parameters see Table 2.

Fig. 10. Intercellular calcium signaling between four cells of configuration J (Fig. 3 J) based on diffusion of both IP_3 and Ca^{2+} through gap junctions. For all parameters see Table 2.

Table 1: Model fluxes

Designation	Dependence	Description	Reference
Fluxes through plasma membrane of cell			
J_{in}	$k_{in} + k_{in}IP_3 \frac{IP_3^2}{K_3^2 + IP_3^2}$	The Ca^{2+} entry through plasma membrane	(Hoefer et al., 2002)
J_{out}	$k_{out}Ca_{cyt}$	The Ca^{2+} extrusion through plasma membrane	(Hoefer et al., 2002)
Fluxes through membrane of endoplasmic reticulum			
J_{rel}	$(k_{leak} + k_{ch}IP_3 \frac{Ca_{cyt}^2}{K_1^2 + Ca_{cyt}^2}) \cdot (Ca_{ER} - Ca_{cyt})$	The Ca^{2+} release from ER	(Marhl et al., 2000)
J_{serca}	$k_{serca}Ca_{cyt}$	The ATPase-mediated Ca^{2+} flux into the ER lumen	(Marhl et al., 2000)
Fluxes through membrane of mitochondria			
J_{mo}	$(k_{mo} \frac{Ca_{cyt}^2}{K_4^2 + Ca_{cyt}^2} + k_m)Ca_m$	The Ca^{2+} release from mitochondria	(Marhl et al., 2000)
J_{mi}	$k_{mi} \frac{Ca_{cyt}^8}{K_2^8 + Ca_{cyt}^8}$	The mitochondrial Ca^{2+} uptake by uniporters	(Marhl et al., 2000)
Interaction of Ca^{2+} with cytosolic calcium binding proteins			
$Ca \implies CaPr$	$k_+ Ca_{cyt} Pr$	The Ca^{2+} binding to proteins	(Marhl et al., 2000)
$CaPr \implies Ca$	$k_- CaPr$	The Ca^{2+} dissociation from proteins	(Marhl et al., 2000)

Table 2: Model parameters

Designation	Parameter values	Description	Reference
Fluxes through plasma membrane of cell			
k_{in}	$0.025\mu M \cdot s^{-1}$	Rate of calcium leak across the plasma membrane	(Hoefer et al., 2002)
k_{out}	$0.5s^{-1}$	Rate constant of calcium extrusion	(Hoefer et al., 2002)
k_{inIP3}	$0.2\mu M \cdot s^{-1}$	Maximal rate of activation-dependent calcium influx	(Hoefer et al., 2002)
K_3	$1\mu M$	Half-saturation constant for agonist-dependent calcium entry	(Hoefer et al., 2002)
Fluxes through membrane of endoplasmic reticulum			
ρ_{ER}	0.01	Volume ratio between the ER and the cytosol	(Marhl et al., 2000)
β_{ER}	0.0025	Ratio of free Ca^{2+} to total Ca^{2+} in the ER	(Marhl et al., 2000)
k_{ch}	$200\mu M^{-1} \cdot s^{-1}$	Maximal permeability of the Ca^{2+} channels in the ER membrane	cf. (Marhl et al., 2000)
k_{serca}	$20s^{-1}$	Rate constant of ATPases	(Marhl et al., 2000)
k_{leak}	$0.05s^{-1}$	Rate constant of Ca^{2+} leak flux through the ER membrane	(Marhl et al., 2000)
K_1	$5\mu M$	Half saturation for Ca^{2+} in ER	(Marhl et al., 2000)
Fluxes through membrane of mitochondria			
ρ_m	0.01	Volume ratio between the mitochondria and the cytosol	(Marhl et al., 2000)
β_m	0.0025	Ratio of free Ca^{2+} to total Ca^{2+} in the mitochondria	(Marhl et al., 2000)
k_{mi}	$300\mu M \cdot s^{-1}$	Maximal rate constant of uniporters in the mitochondrial membrane	(Marhl et al., 2000)
k_{mo}	$125s^{-1}$	Maximal rate for Ca^{2+} flux through Na^+/Ca^{2+} exchangers and PTPs	(Marhl et al., 2000)
k_m	$0.00625s^{-1}$	Rate constant of the non-specific leak flux	(Marhl et al., 2000)
K_4	$5\mu M$	Half saturation for Ca^{2+} in mitochondria	(Marhl et al., 2000)
K_2	$0.8\mu M$	Half saturation for Ca^{2+} of uniporters in the mitochondrial membrane	(Marhl et al., 2000)
Interaction of Ca^{2+} with cytosolic calcium binding proteins			

k_+	$0.1\mu M^{-1} \cdot s^{-1}$	On rate constant of Ca^{2+} binding to proteins	(Marhl et al., 2000)
k_-	$0.01s^{-1}$	Off rate constant of Ca^{2+} binding to proteins	(Marhl et al., 2000)
Pr_{tot}	$120\mu M$	Total concentration of free and bounded Ca^{2+} -binding sites on the cytosolic proteins	(Marhl et al., 2000)
Gap junctions between cells			
k_G	$0.4\mu M$	Half saturation for all second messengers in gap junctions	cf. (Lazrak et al., 1994)
$k_{Ca(ij)}$	$0.4\mu M$	Permeability of gap junctions between cells i and j for Ca^{2+}	cf. (Lazrak et al., 1994)
$k_{IP(ij)}$	$0.16\mu M$	Permeability of gap junctions between cells i and j for IP_3	cf. (Lazrak et al., 1994)
k_{gap}	$1s^{-1}$	Rate constant of propagation Ca^{2+} and IP_3 through gap junctions between cells i and j	cf. (Lazrak et al., 1994)
Degradation of IP_3			
k_p	$1\mu M$	Half saturation for IP_3 degradation	(Sneyd et al., 1995)
V_p	$0.01s^{-1}$	Rate constant of IP_3 degradation	cf. (Sneyd et al., 1995)

Table 3: Intercellular calcium waves in different configurations of four cells

	Cell 1	Cell 2	Cell 3	Cell 4
Configuration A, $\gamma_{Ca(14)} = 0, \gamma_{IP(14)} = 0$				
Duration of oscillatory behavior of Ca_{cyt} , (s)	536.1	452.5	452.5	402.8
Delay time of Ca_{cyt} from the first cell, (s)	0	83.6	83.8	133.3
Number of oscillations of Ca_{cyt}	8	7	7	6
Amplitude of the first/the last oscillation of Ca_{cyt} , (μM)	0.85/0.68	0.76/0.6	0.76/0.6	0.75/0.6
Amplitude of IP_3 , (μM)	18.7	6.4	6.4	5.4
Location of maximum of IP_3 , (s)	260	326.7	326.7	386.5
Configuration B, $\gamma_{Ca(23)} = 0, \gamma_{IP(23)} = 0$				
Duration of oscillatory behavior of Ca_{cyt} , (s)	488.6	413.8	413.8	413.8
Delay time of Ca_{cyt} from the first cell, (s)	0	74.8	74.8	74.8
Number of oscillations of Ca_{cyt}	8	7	7	7
Amplitude of the first/the last oscillation of Ca_{cyt} , (μM)	0.85/0.6	0.75/0.6	0.75/0.6	0.75/0.6
Amplitude of IP_3 , (μM)	15.65	6.35	6.35	6.35
Location of maximum of IP_3 , (s)	260	325	325	325
Configuration C, $\gamma_{Ca(13)} = 0, \gamma_{IP(13)} = 0, \gamma_{Ca(14)} = 0, \gamma_{IP(14)} = 0$				
Duration of oscillatory behavior of Ca_{cyt} , (s)	146.7	286.5	106.5	106.5
Delay time of Ca_{cyt} from the first cell, (s)	0	91.7	271.7	271.7
Number of oscillations of Ca_{cyt}	6	3	2	2
Amplitude of the first/the last oscillation of Ca_{cyt} , (μM)	0.83/0.69	0.75/0.64	0.66/0.64	0.66/0.64
Amplitude of IP_3 , (μM)	23	6.5	4.2	4.2
Location of maximum of IP_3 , (s)	260	330	397	397
Configuration D, $\gamma_{Ca(14)} = 0, \gamma_{IP(14)} = 0, \gamma_{Ca(24)} = 0, \gamma_{IP(24)} = 0$				
Duration of oscillatory behavior of Ca_{cyt} , (s)	433	372	372	191.7
Delay time of Ca_{cyt} from the first cell, (s)	0	61	61	241.3
Number of oscillations of Ca_{cyt}	7	6	6	4
Amplitude of the first/the last oscillation of Ca_{cyt} , (μM)	0.84/0.6	0.77/0.6	0.77/0.6	0.68/0.6
Amplitude of IP_3 , (μM)	18.75	6.5	6.4	4.3

Location of maximum of IP_3 , (s)	260	325	327	400
Configuration E, $\gamma_{Ca(23)} = 0$, $\gamma_{IP(23)} = 0$, $\gamma_{Ca(24)} = 0$, $\gamma_{IP(24)} = 0$				
Duration of oscillatory behavior of Ca_{cyt} , (s)	492	416	416	416
Delay time of Ca_{cyt} from the first cell, (s)	0	76	76	76
Number of oscillations of Ca_{cyt}	8	7	7	7
Amplitude of the first/the last oscillation of Ca_{cyt} , (μM)	0.85/0.6	0.75/0.6	0.75/0.6	0.75/0.6
Amplitude of IP_3 , (μM)	15.65	6.35	6.35	6.35
Location of maximum of IP_3 , (s)	260	325	325	325
Configuration F, $\gamma_{Ca(23)} = 0$, $\gamma_{IP(23)} = 0$, $\gamma_{Ca(24)} = 0$, $\gamma_{IP(24)} = 0$, $\gamma_{Ca(34)} = 0$, $\gamma_{IP(34)} = 0$				
Duration of oscillatory behavior of Ca_{cyt} , (s)	492	416	416	416
Delay time of Ca_{cyt} from the first cell, (s)	0	76	76	76
Number of oscillations of Ca_{cyt}	8	7	7	7
Amplitude of the first/the last oscillation of Ca_{cyt} , (μM)	0.85/0.6	0.75/0.6	0.75/0.6	0.75/0.6
Amplitude of IP_3 , (μM)	15.65	6.35	6.35	6.35
Location of maximum of IP_3 , (s)	260	325	325	325
Configuration G, $\gamma_{Ca(13)} = 0$, $\gamma_{IP(13)} = 0$, $\gamma_{Ca(14)} = 0$, $\gamma_{IP(14)} = 0$, $\gamma_{Ca(34)} = 0$, $\gamma_{IP(34)} = 0$				
Duration of oscillatory behavior of Ca_{cyt} , (s)	155	223	162.5	162.5
Delay time of Ca_{cyt} from the first cell, (s)	0	96.8	157.37	157.37
Number of oscillations of Ca_{cyt}	6	3	2	2
Amplitude of the first/the last oscillation of Ca_{cyt} , (μM)	0.83/0.7	0.77/0.67	0.7/0.67	0.7/0.67
Amplitude of IP_3 , (μM)	23	6.5	4.17	4.17
Location of maximum of IP_3 , (s)	260	330	397	397
Configuration H, $\gamma_{Ca(14)} = 0$, $\gamma_{IP(14)} = 0$, $\gamma_{Ca(23)} = 0$, $\gamma_{IP(23)} = 0$				
Duration of oscillatory behavior of Ca_{cyt} , (s)	464.5	384.5	384.5	331
Delay time of Ca_{cyt} from the first cell, (s)	0	80	80	133.5
Number of oscillations of Ca_{cyt}	8	7	7	6
Amplitude of the first/the last oscillation of Ca_{cyt} , (μM)	0.85/0.6	0.77/0.6	0.77/0.6	0.77/0.6
Amplitude of IP_3 , (μM)	18.7	6.3	6.3	5.4

Location of maximum of IP_3 , (s)	260	325	325	387
Configuration I, $\gamma_{Ca(13)} = 0$, $\gamma_{IP(13)} = 0$, $\gamma_{Ca(14)} = 0$, $\gamma_{IP(14)} = 0$, $\gamma_{Ca(24)} = 0$, $\gamma_{IP(24)} = 0$				
Duration of oscillatory behavior of Ca_{cyt} , (s)	145.8	59.5	59	—
Delay time of Ca_{cyt} from the first cell, (s)	0	61.5	61.8	—
Number of oscillations of Ca_{cyt}	6	2	2	0
Amplitude of the first/the last oscillation of Ca_{cyt} , (μM)	0.85/0.69	0.77/0.74	0.02/0.04	—
Amplitude of IP_3 , (μM)	23	8.3	3.95	2.4
Location of maximum of IP_3 , (s)	260	340	393	463
Configuration J, $\gamma_{Ca(14)} = 0$, $\gamma_{IP(14)} = 0$, $\gamma_{Ca(23)} = 0$, $\gamma_{IP(23)} = 0$, $\gamma_{Ca(24)} = 0$, $\gamma_{IP(24)} = 0$				
Duration of oscillatory behavior of Ca_{cyt} , (s)	483.5	426.8	377	234.5
Delay time of Ca_{cyt} from the first cell, (s)	0	56.7	111	261.2
Number of oscillations of Ca_{cyt}	8	8	6	4
Amplitude of the first/the last oscillation of Ca_{cyt} , (μM)	0.85/0.6	0.8/0.6	0.74/0.6	0.67/0.6
Amplitude of IP_3 , (μM)	18.7	8.2	6.05	3.83
Location of maximum of IP_3 , (s)	260	335	314	396

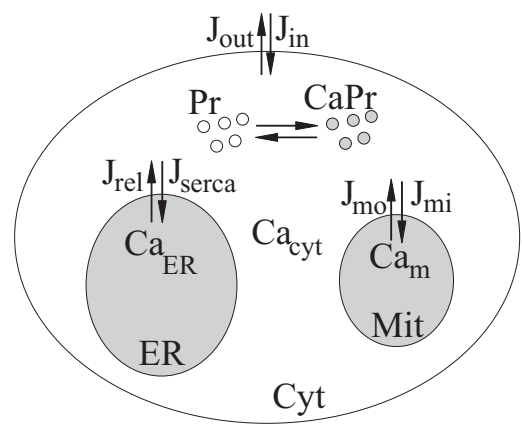


Fig. 1.

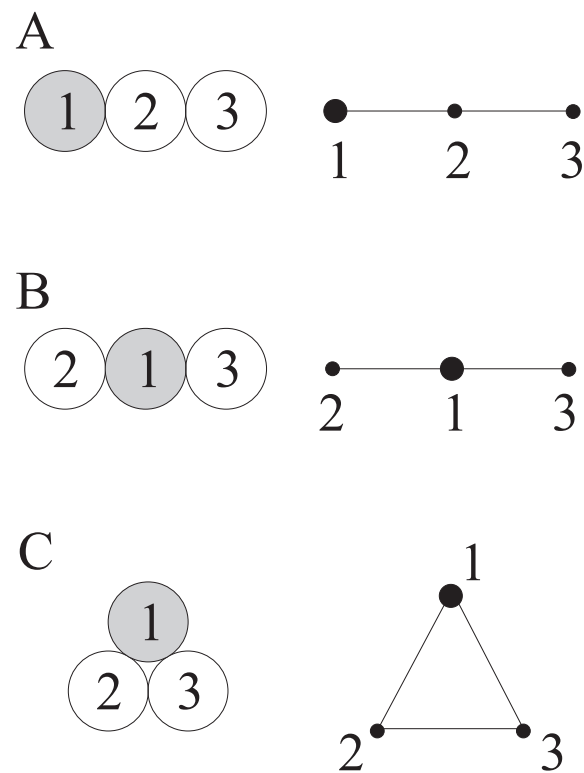


Fig. 2.

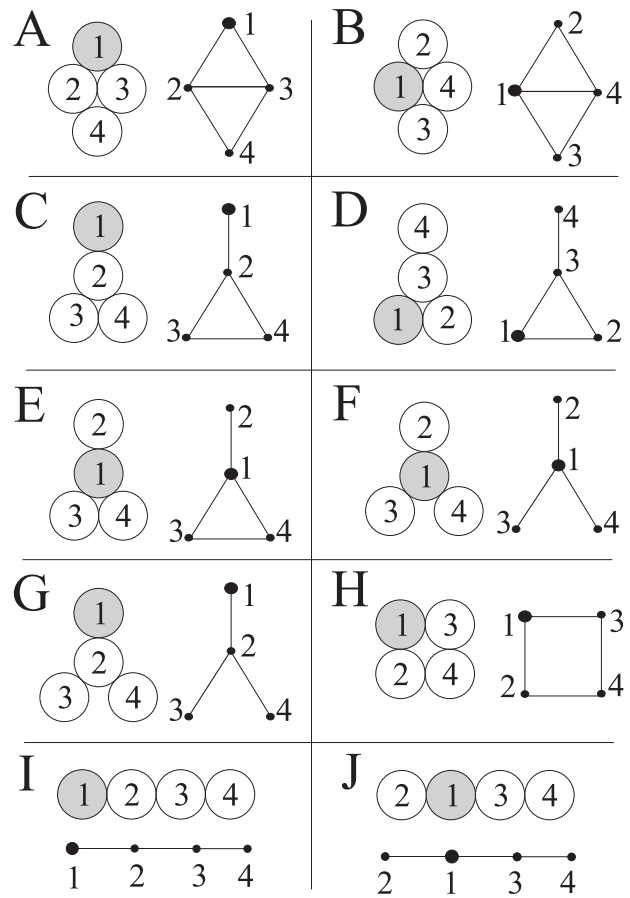


Fig. 3.

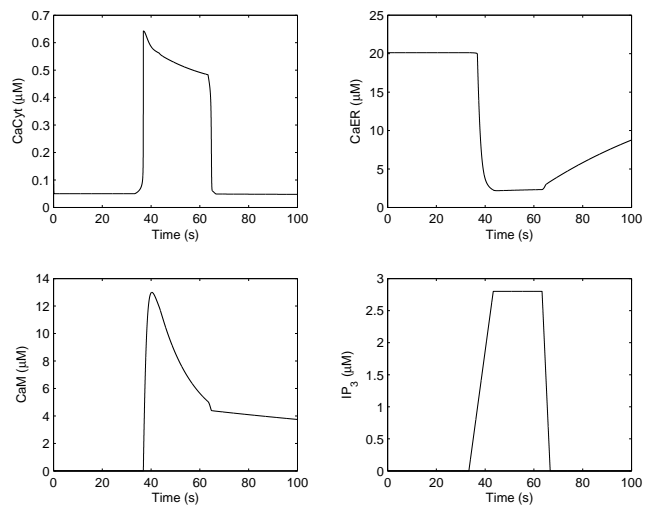


Fig. 4.

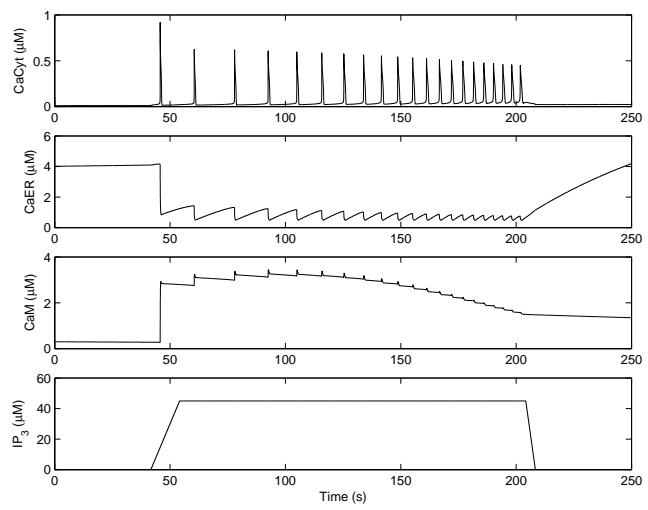


Fig. 5.

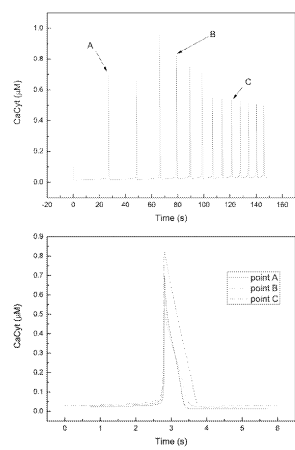


Fig. 6.

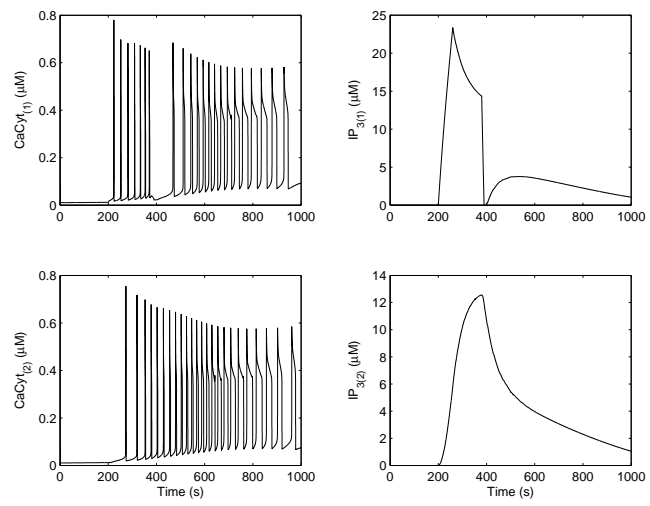


Fig. 7.

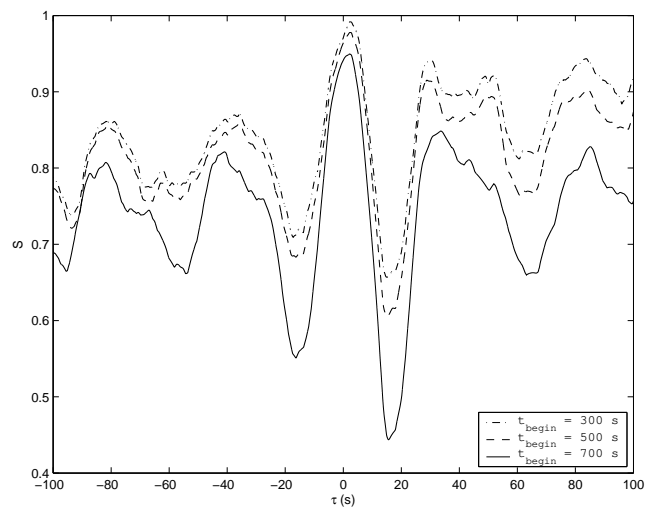


Fig. 8.

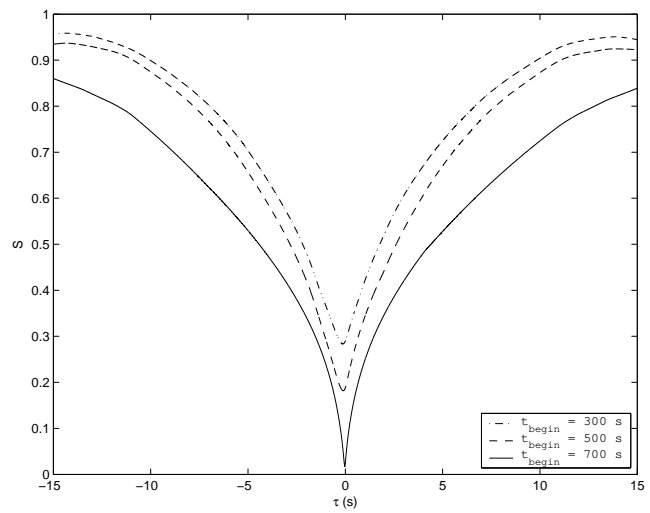


Fig. 9.

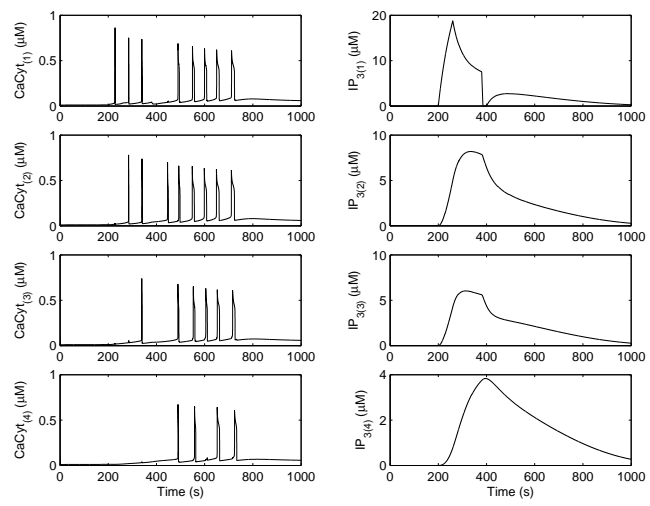


Fig. 10.